Am J Cancer Res 2024;14(6):2881-2893
www.ajcr.us /ISSN:2156-6976/ajcr0156607

Original Article

αPD-1 immunotherapy promotes IL-17A production and promotes the formation of acute radiation-induced lung injury

Shilong Liu*, Lili Liu*, Jianli Ma, Jian Li, Liqun Wang, Jianyu Xu, Songliu Hu

*Department of Radiation Oncology, Harbin Medical University Cancer Hospital, Harbin 150081, Heilongjiang, China. *Equal contributors.*

Received March 16, 2024; Accepted May 29, 2024; Epub June 15, 2024; Published June 30, 2024

Abstract: Background: Radiotherapy (RT) is essential in the treatment of thoracic neoplasms. Immune checkpoint inhibitors targeting programmed cell death protein 1 (PD-1) and programmed death-ligand 1 (PD-L1) have significantly improved the clinical management of non-small cell lung carcinoma (NSCLC). Objective: This study aimed to investigate the impact of combining anti-PD-1 (αPD-1) immunotherapy with radiotherapy on lung injury. Additionally, it investigates the role and mechanism of interleukin (IL)-17A, a pro-inflammatory cytokine involved in immune regulation, in lung injury arising from this combination treatment. Methods: Experiments were conducted using a PD-1 deficient mouse model to simulate acute radiation-induced lung injury. Inbred female BALB/c wild-type (WT) mice and PD-1$^{-/-}$ mice were divided into six groups: WT group, PD-1$^{-/-}$ group, WT_LIR + IgG group, PD-1$^{-/-}$_LIR + IgG group, WT_LIR + αIL-17A group, and PD-1$^{-/-}$_LIR + αIL-17A group. The mice were subjected to 8 Gy × 3 irradiation in both lungs. Various methods including histological scoring, immunofluorescence, qPCR, and flow cytometry were employed to analyze the role of IL-17A in lung injury and the effect of PD-1 gene deletion on the severity of radiation-induced lung injury. Results: The PD-1$^{-/-}$_LIR mice exhibited evident radiation-induced lung injury after receiving 8 Gy × 3 doses in both lungs. The expression level of IL-17A peaked at 2 weeks. Lung injury-related factors IFN-γ, TNF-α, IL-6, and RORγt in the PD-1$^{-/-}$_LIR groups increased 2 weeks after irradiation. The CD4$^+$ and CD8$^+$ T cells in lung tissue of the PD-1$^{-/-}$_LIR mice significantly increased. Post αIL-17A administration, the incidence of alveolitis in the treatment group decreased, the expression levels of lung injury-related factors IFN-γ, TNF-α, IL-6, RORγt, TGF-β1, and IL-17A decreased, and the CD4$^+$ and CD8$^+$ T cells in lung tissue significantly declined. Throughout the observation period, the survival rate of the mice in the treatment group was significantly higher than that of the isotype control group (60% vs 0%, P = 0.011). Conclusion: Combining αPD-1 immunotherapy with radiotherapy in mice can induce radiation-induced lung injury, with IL-17A playing a critical role in this process. αIL-17A administration significantly mitigated radiation-induced lung injury caused by the combination of αPD-1 immunotherapy and radiotherapy, improving mouse survival. This finding offers a promising treatment target for lung injury resulting from the combination of αPD-1 immunotherapy and radiotherapy.

Keywords: αPD-1, IL-17A, acute radiation, lung injury, immunotherapy

Introduction

Radiotherapy (RT) essential in the treatment of thoracic neoplasms [1]. However, radiation-induced lung injury (RILI) can lead to complications such as cough, shortness of breath, panting, or respiratory failure, limiting the dose of thoracic RT [2-4]. Immune checkpoint inhibitors targeting programmed cell death protein 1 (PD-1) and programmed death-ligand 1 (PD-L1) have significantly improved the clinical management of non-small cell lung carcinoma (NSCLC) [5]. The combination of RT with PD-1/PD-L1 blockade has remarkably improved the overall survival (OS) and progression-free survival (PFS) rates among NSCLC patients [6, 7]. However, the impact of concurrent anti-PD-1 (αPD-1) therapy and RT on non-malignant lung tissue toxicity has not been thoroughly investigated in clinical studies. Therefore, investigat-

https://doi.org/10.62347/WDOC4830

ing the potential risks and benefits of this combined therapy is essential to refine the clinical outcomes of NSCLC patients.

αPD-1 therapy has demonstrated efficacy in treating lung cancer by blocking the PD-1/PD-L1 interaction and enhancing the immune response against cancer cells. Several clinical trials have established the efficacy of αPD-1 therapy in treating NSCLC. For example, in the phase III clinical trial KEYNOTE-024, pembrolizumab, an αPD-1 therapy, was found to be superior to standard chemotherapy in treating NSCLC with high PD-L1 expression [8]. Furthermore, radiotherapy can enhance the immunogenicity of tumors by promoting tumor cell death and the release of tumor antigens, which can serve as targets for immune cells, triggering anti-tumor immune responses. In addition to these advancements, several recent clinical trials have made notable contributions to the field. The "Pacific" trial, for example, investigated the efficacy of combining radiotherapy with the PD-L1 antibody durvalumab in NSCLC patients. The results showed a significant improvement in PFS compared to radiotherapy alone, leading to the approval of durvalumab as a standard treatment for locally advanced NSCLC patients who are not eligible for surgical resection [9]. Another significant clinical trial, the "Keylynk" study, explored the combination of radiotherapy and the αPD-1 antibody pembrolizumab as a treatment for advanced NSCLC patients. Preliminary results demonstrated substantial improvements in PFS and OS, providing important evidence for the further application of this treatment strategy [10]. Additionally, the "Keynote-799" trial assessed the efficacy of combining radiotherapy with pembrolizumab on advanced NSCLC [11]. In conclusion, recent clinical trials such as "Pacific", "Keylynk", and "Keynote-799" have further validated the potential of combined radiotherapy and immunotherapy in the treatment of lung cancer, offering new avenues for improving patient outcomes and revolutionizing cancer treatment strategies.

The combination of αPD-1 immunotherapy and radiotherapy has emerged as an effective treatment for certain cancers. However, this treatment can induce lung injury as an adverse side effect [12]. The underlying mechanism is not fully understood, but it is thought to be related to the immune response elicited by the treatment, which can cause inflammation. Studies have suggested that IL-17A, a cytokine that promotes inflammation, may contribute to the development of lung injury induced by αPD-1 immunotherapy combined with radiotherapy [13]. Abhishek et al. summarized in a review that IL-17A may enhance the infiltration of inflammatory cells and increase oxidative stress in lung tissue, resulting in lung injury [14]. Furthermore, IL-17A may impair the efficacy of αPD-1 immunotherapy, increasing the risk of tumor cells evading from immune surveillance and causing lung injury. To mitigate the risk of lung injury, physicians are advised to closely monitor patients for signs of lung injury during treatment and adjust treatment protocols as needed. In some cases, treatment may need to be temporarily or permanently discontinued to prevent further lung damage.

The aim of this study is to investigate the role and mechanism of interleukin (IL)-17A in preventing lung injury induced by deletion of the PD-1 gene and radiotherapy. IL-17A is a cytokine that promotes inflammation and regulates immune cell function. High levels of IL-17A can cause inflammation and oxidative stress in lung tissue, leading to lung injury [15]. Additionally, IL-17A can reduce the effectiveness of PD-1 immunotherapy and increase the ability of tumor cells to escape immune attack [16]. Therefore, understanding the role and mechanism of IL-17A in preventing lung injury induced by PD-1 immunotherapy and radiotherapy is crucial for developing more effective protective measures.

Methods

Radiation schedule

This study was approved by Harbin Medical University Cancer Hospital. 6 to 8-week-old female BALB/c mice, both wild-type (WT) and PD-1$^{-/-}$ mice models were purchased from Beijing Vitonglihua Experimental Animal Technology Co., LTD. The mice were housed in a specific pathogen-free (SPF) facility. For the radiation exposure, were immobilized the mice on a linear accelerator (Xstrahl, UK) and scanned using cone-beam computed tomography with the small animal radiation research platform (SARRP) under anesthesia (pentobarbital sodium, 30-90 mg/kg; i.p.). The CT

Table 1. The sequence of primers

Gene	Forward sequence (5'-3')	Reverse sequence (5'-3')
IL-17A	TCCCTCTGTGATCTGGGAAG	AGCATCTTCTCGACCCTGAA
β-actin	TCCTTCGTTGCCGGTCCACCA	ACCAGCGCAGCGATATCGTCTC
IFN-γ	AACGCTACACACTGCATCTTGGG	GCCGTGGCAGTAACAGCCGCC
IL-6	GGCCCTTGCTTTCTCTTCG	ATAATAAAGTTTTGATTATGT
IL-1β	CACAGCAGCACATCAACAAG	GTGCTCATGTCCTCATCCTG
RORγt	CCTGGGCTCCTCGCCTGACC	TCTCTCTGCCCTCAGCCTTGCC
TGF-β1	GGCCAGATCCTGTCCAAGC	GTGGGTTTCCACCATTAGCAC
TNF-α	GGTGCCTATGTCTCAGCCTCTT	GCCATAGAACTGATGAGAGGGAG

images were then used to develop a treatment plan using the Muriplan (Camberley, UK) treatment planning system for contouring of the lung tissues. An eight-field conformal radiation therapy technique was used to treat both lungs, and the treatment plan was transferred to the treatment system. The mice underwent radiation therapy using a single high-dose fractionation approach, with each fraction delivering 8 Gy, for a total of three fractions. Control mice were exposed to 0 Gy using the same procedure. WT and PD-1$^{-/-}$ mice were randomly divided into six groups after a 7-day adaptation period: (1) WT group; (2) WT_LIR + IgG group with bilateral lung irradiation of 8 Gy × 3 under anesthesia; (3) PD-1$^{-/-}$ group; (4) PD-1$^{-/-}$_LIR + IgG group; (5) WT_LIR + αIL-17A group; (6) PD-1$^{-/-}$_LIR + αIL-17A group. Additionally, WT mice and PD-1$^{-/-}$ mice were prepared to investigate the effects and mechanisms of IL-17A blockade in combination with αPD-1 immunotherapy and radiation-induced lung injury. These mice were divided into six groups and their survival times were observed.

The mice received intraperitoneal injections one day prior to irradiation and twice a week for four consecutive weeks. These injections included either 200 μg of immunoglobulin G (IgG) isotype or αIL-17A (Bio X Cell, clone: 17F3, catalog number BP0173) dissolved in 200 μl of physiological saline to maintain circulating levels.

Histological analysis

Mice were humanely euthanized using carbon dioxide (CO_2) asphyxiation on days 7, 14, 28, and 56 following the initial exposure to irradiation. The left lungs were fixed, embedded in paraffin, and sectioned for hematoxylin and eosin (HE) staining. The pathological grades of injury were assessed blindly by two independent investigators using the criteria outlined in previous reports: 0 = no lung abnormality, 1 = inflammation involving less than 25% of the lung parenchyma, 2 = lesions involving 25-50% of the lung, 3 = lesions involving more than 50% of the lung [17, 18]. The mean pathological grade for each mouse was determined from two sections. Histological analysis of the lungs was conducted as described [19].

RNA isolation and real-time polymerase chain reaction (PCR)

Total RNA was extracted from the lung tissues using TRI Reagent® (Sigma, cat#T9424) following the manufacturer's protocol. The cDNA was synthesized using High-Capacity cDNA Reverse Transcription Kit (Applied Biosystems™, cat#4368814). The primer sequences are listed in **Table 1**. Quantification was performed using SYBR™ Green PCR Master Mix (Applied Biosystems™, cat#4309155). Each sample was determined in triplicates. The relative mRNA levels were calculated based on β-actin according to the report.

Cell preparation from lung organs

The lungs of the mice were cut into small pieces and digested in 1 mg/mL collagenase D (Roche, Basel, Switzerland) and 40 U/mL DNase I (Roche, Basel, Switzerland) for 30 minutes at 37°C while shaking. After digestion, 10 mM EDTA was added to stop the enzymatic process. The lung and spleen tissues were triturated and filtered through 70 μm cell strainers. Erythrocytes were lysed in red blood cell lysing buffer (Sigma-Aldrich, St Louis, MO, USA).

The resulting single-cell suspensions were washed twice in phosphate-buffered saline

(PBS) and resuspended in fluorescence-activated cell sorting (FACS) buffer (PBS containing 2% fetal bovine serum). Flow-cytometric analyses of lung tissue were performed using specific antibodies against CD3 (labeled with CY7, clone: 17A2), CD8a (labeled with FITC, clone: YTS169.4), and CD4 (labeled with APC/CY5.5, clone: GK1.5), which were obtained from BioLegend. The samples were then analyzed using a CytoFLEX S flow cytometer from Beckman Coulter. The FACS results were analyzed using FlowJo software, version 10.4.0 (RRID: SCR_008520).

Immunostaining

Lungs were cryopreserved and cut into 6 μm thick sections. Frozen sections were fixed with 4% paraformaldehyde for 30 minutes. Staining was performed with IL17A (ab79056 from abcam), anti-CD4 (GK1.5 from Thermo Scientific) and anti-CD8a (ab270926 from abcam). The stained slides were subsequently imaged using an Applied biosystems microscope.

Gene Ontology (GO) and Kyoto Encyclopaedia of Genes and Genomes (KEGG) pathway enrichment analyses

The GO and KEGG enrichment were performed on the Database for Metascape (https://metascape.org). The KEGG enrichment analysis reveals potential biological processes with critical targets. The bioinformatics platform (https://www.bioinformatics.com.cn/) was used to generate the bubble chart of GO and KEGG enrichment analyses.

Tumor infiltration analysis

Tumor Immune Estimation Resource (TIMER) database (https://cistrome.org/TIMER/) [20, 21], a database of immune cells that infiltrate tumors, was used to investigate immune cell infiltration into tumors. The TIMER database uses TCGA data to analyze gene expression associations between cancer and immune infiltration. The correlation coefficients for gene expression were calculated with Spearman's correlation and displayed as log2 RSEM.

Statistical analysis

All analyses were performed using GraphPad Prism version 7.0 (RRID: SCR_002798). The unpaired two-tailed Student's t-test was used for two-group comparison. One-way ANOVA with Dunnett (for comparing each group to control group) or Tukey (for comparisons between every two groups) was used to compare multiple groups. Survival data were compared using the log-rank test. $P < 0.05$ was considered significant.

Results

Role of IL-17A in lung cancer revealed by KEGG pathway enrichment analysis and its significant alteration post anti-PD-1 therapy

According to an extensive literature review conducted by Abhishek et al. [14], a total of 34 genes related to Immunogenic Cell Death (ICD) were identified and filtered. These genes, including ATG5, BAX, CALR, CASP1, CASP8, CD4, CD8A, CD8B, CXCR3, EIF2AK3, ENTPD1, FOXP3, HMGB1, HSP90AA1, IFNA1, IFNB1, IFNG, IFNGR1, IL10, IL17A, IL17, RAIL1B, IL1R1, IL6, LY96, MYD88, NLRP3, NT5E, P2RX7, PDIA3, PIK3CA, PRF1, TLR4, and TNF, were analyzed using bioinformatics tools and Metascape, including the Kyoto Encyclopedia of Genes and Genome (KEGG), pinpointing IL-17A pathway as a critical component in lung cancer, particularly in lung adenocarcinoma (LUAD) samples from The Cancer Genome Atlas (TCGA) database (**Figure 1**) [22].

The absence of PD-1 exacerbated acute radiation-induced lung injury (RILI). We subjected the thoracic area of WT or PD-1$^{-/-}$ mice to 8 Gy × 3 irradiation treatment (**Figure 2A**). The irradiated mice were monitored for 56 days. Histopathological evaluation of lung tissue damage post irradiation showed a time-dependent increase in tissue injury. On day 14, observations included alveolar collapse, lung capillary hyperemia, hemorrhage, and inflammatory exudate (**Figure 2B**). The percentage of pulmonary inflammatory lesions was calculated, and histological scoring criteria for RILI were used [23]. RILI histological score was higher in the irradiated mice compared to those treated with irradiation plus isotype (**Table 2**). Inflammatory cell infiltration increased on days 14 and 28 post-irradiation, along with thickened alveolar septum, with PD-1$^{-/-}$ mice exhibiting a more severe response (**Figure 2B**).

Based on H&E staining (**Figure 2B**) and lung inflammation score results (**Table 2**), treatment

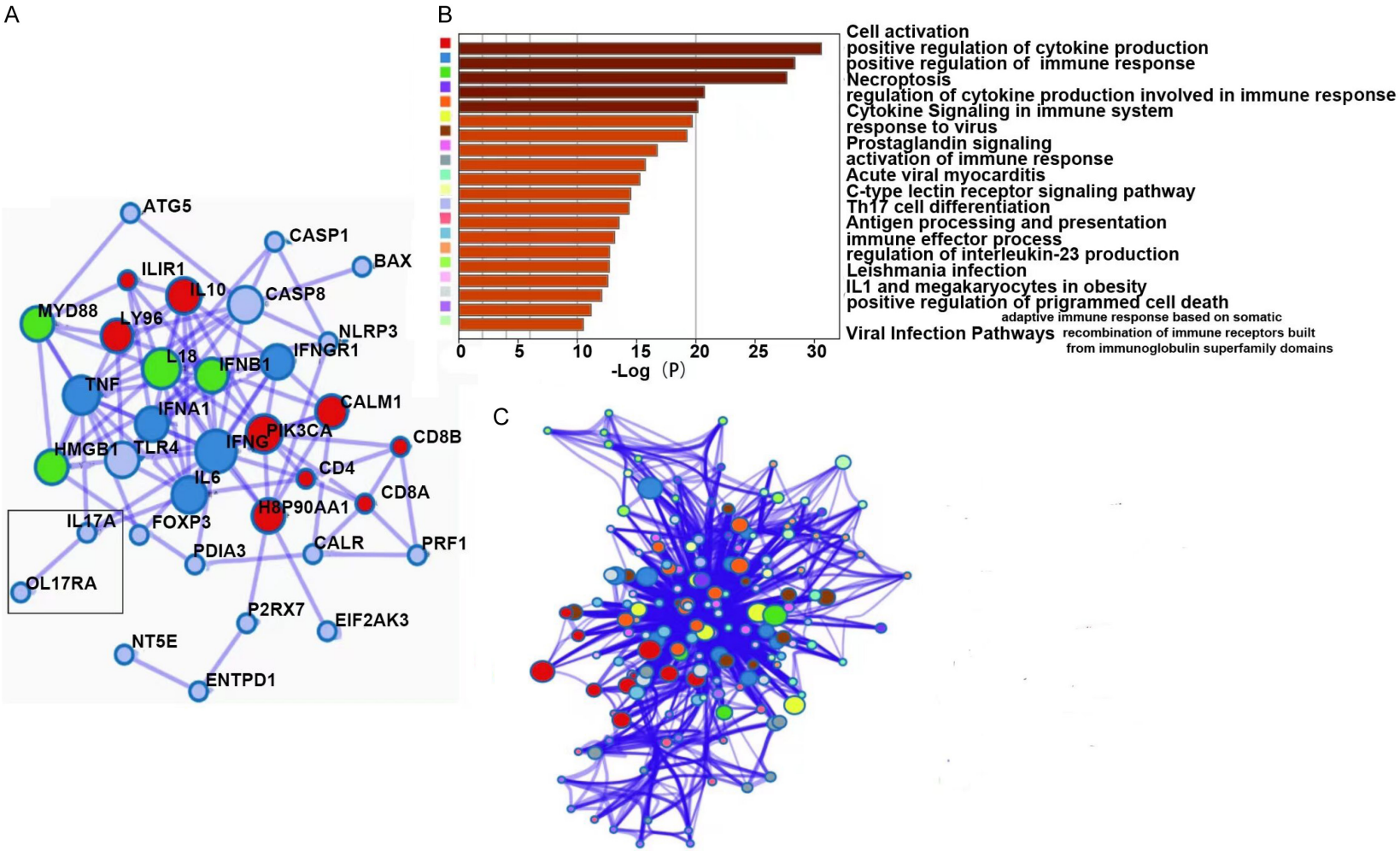

Figure 1. Pathway analysis of 34 ICD-related genes in cancer patients. A. Functional network analysis conducted using GeNet reveals several distinct communities. B. Gene Ontology (GO) processes enriched analysis. C. GO terms enriched using the ClueGO Cytoscape plug-in. The above results were analyzed using Metascape.

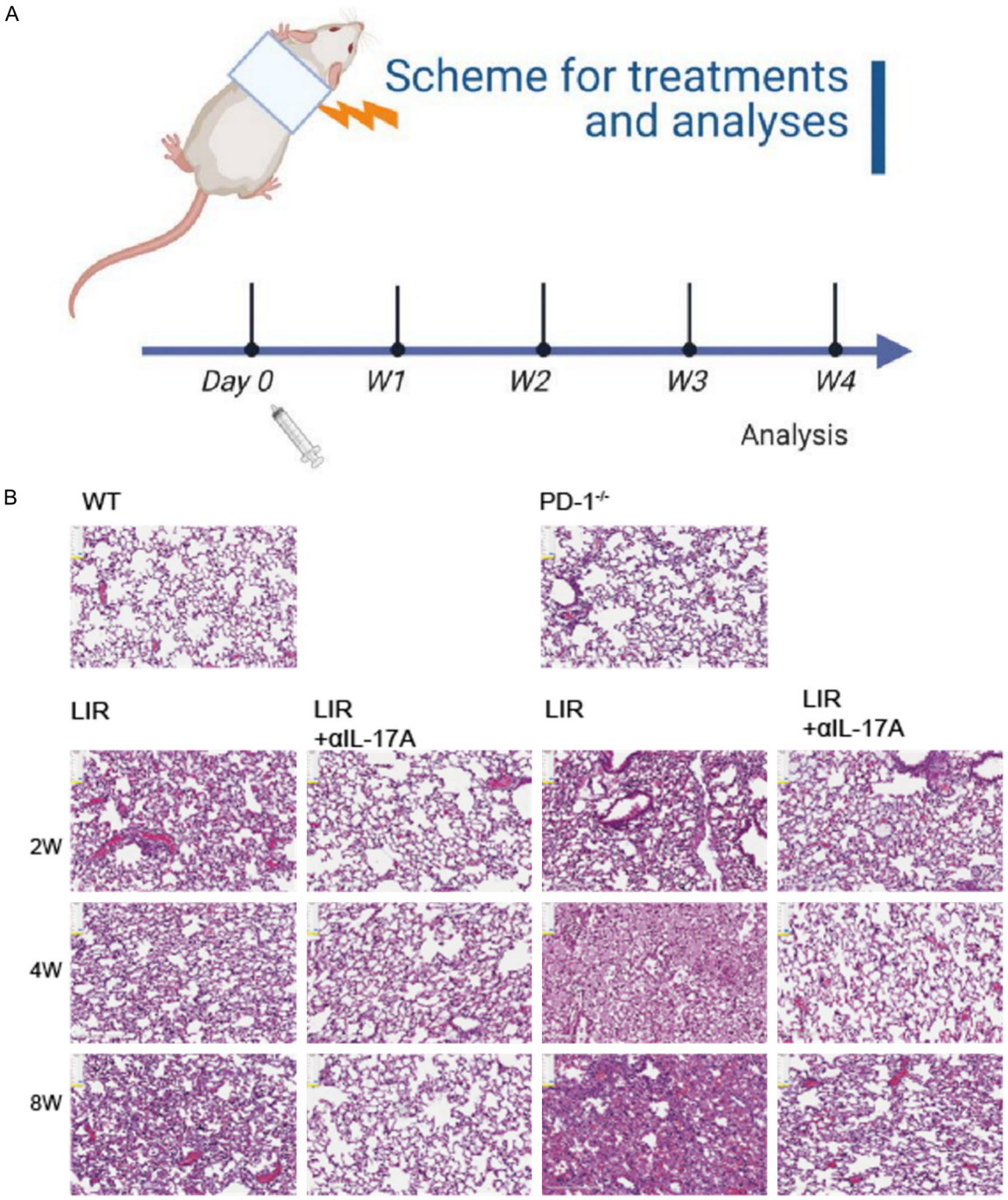

Figure 2. Scheme for treatments and analyses of the animal model. A. Illustration depicting the treatment scheme and experimental setup for the animal model. The mice received a total of 8 Gy × 3 irradiation focused on the thoracic area. The treatment involved a combination of radiotherapy and αIL-17A administration. Analyses were performed at specified time points post-irradiation to evaluate lung tissue changes and immune responses. B. Pathological changes in Lung. Tissue in different groups post-radiotherapy (H&E Staining, 20 × Magnification).

with αIL-17A effectively mitigated the severity of mouse lung inflammation. Pathological changes in lung tissues were significantly reduced in the PD-1$^{-/-}$_LIR + αIL-17A group at 4 weeks, with only mild thickening of alveolar septa and destruction of alveolar structures observed.

Table 2. Comparison of the degree of radiation-induced lung injury in each group after IL-17A antibody according to Szapiel scoring system (4W)

Group	N	Szapiel scoring system			
		0	I	II	III
WT	20	20	0	0	0
PD-1$^{-/-}$	20	18	2	0	0
WT_LIR + IgG	20	0	6	10	4
PD-1$^{-/-}$_LIR + IgG*	20	0	4	4	12
WT_LIR + αIL-17A	20	0	10	8	2
PD-1$^{-/-}$_LIR + αIL-17A**	20	0	8	8	4

*P < 0.05 PD-1$^{-/-}$_LIR + IgG vs WT_LIR + IgG; **P < 0.05 PD-1$^{-/-}$_LIR + αIL-17A vs PD-1$^{-/-}$_LIR + IgG.

Notably, lung inflammation in the PD-1$^{-/-}$_LIR + αIL-17A group was significantly alleviated compared to that in the PD-1$^{-/-}$_LIR + IgG group.

Subsequently, we used qPCR and immunofluorescence to detect the expression of IL-17A in mouse lung tissue after irradiation. qPCR results indicated a significant increase in IL-17A expression after irradiation, with higher expression levels observed in the PD-1$^{-/-}$ group compared to the WT group (**Figure 3**).

These findings suggest that the loss of the PD-1 gene leads to an increase in IL-17A expression, emphasizing the critical role of KEGG and other methods in filtering out the IL17A pathway. Additionally, the results hint at the exacerbated acute RILI experienced by PD-1$^{-/-}$ mice and the significant alleviation provided by αIL-17A treatment.

Analysis of immune-related factors, cell infiltration in mouse lung tissue post-radiotherapy

IL-17A is a potent stimulant that triggers various cell types to product pro-inflammatory cytokines and attracts T cells, notably CD4$^+$ and CD8$^+$ T cells, thereby establishing an IL-17A-driven cytokine network that actively participates in inflammation [12, 15]. In this study, we employed the TIMER database to compute the Spearman correlation between the expression of CD4$^+$ and CD8$^+$ T cell infiltration. The results revealed a non-significant (P > 0.05) infiltration of CD4$^+$ and CD8$^+$ T immune cells in lung cancers (**Figure 4A**).

Subsequently, we evaluated the levels of inflammatory cytokines and associated T cells. Firstly, we investigated the infiltration of CD4$^+$ and CD8$^+$ T cells in mouse lung tissue at 2 weeks post-radiotherapy using immunofluorescence (**Figure 4B**) and flow cytometry (**Figure 4C**). In unirradiated mice, there was no significant difference in the total number of CD8$^+$ or CD4$^+$ T cells in lung tissue between the WT and PD-1$^{-/-}$ mice (**Figure 4B**). However, following radiation treatment, there was a significant increase in the total number of CD8$^+$ or CD4$^+$ T cells in the lung tissue of both WT and PD-1$^{-/-}$ mice, with a more pronounced infiltration in PD-1$^{-/-}$ mice (**Figure 4B**, **4C**). Moreover, flow cytometry analysis demonstrated a significant difference in CD4$^+$ or CD8$^+$ T cells between untreated mice and the other groups (**Figure 4C**). Our results indicate that radiation therapy induces the secretion of substantial amounts of inflammatory cytokines and chemokines in mouse lung tissue, leading to the recruitment of a considerable proportion of CD8$^+$ or CD4$^+$ T cells.

We further examined the expression of inflammation-related factors in lung tissue post-irradiation. Through qPCR, we observed an upregulation of inflammatory cytokines and chemokines, including IFN-γ, TNF-α, IL-6, RORγt, TGF-β1, and IL-17A. Interestingly, this upregulation was more pronounced in PD-1$^{-/-}$ mice than in the WT group (**Figure 5**).

Furthermore, we investigated the expression of inflammation-related factors in lung tissue after irradiation under the influence of αIL-17A. Employing qPCR, we observed a decrease in the expression of inflammatory cytokines and chemokines, including IFN-γ, TNF-α, IL-6, RORγt, TGF-β1, and IL-17A (**Figure 5**). Moreover, αIL-17A significantly reduced the infiltration of CD8$^+$ or CD4$^+$ T cells in the lung tissue of WT and PD-1$^{-/-}$ mice after radiation treatment (**Figure 4B**). Flow cytometry analysis also indicated a reduction in the percentage of CD8$^+$ or CD4$^+$ T cells in PD-1$^{-/-}$_LIR + αIL-17A mice (**Figure 4C**).

Mouse survival curves indicated no significant difference in survival between WT mice and PD-1$^{-/-}$ mice. However, following radiation therapy, the PD-1$^{-/-}$ mice exhibited a significantly reduced survival rate. The addition of αIL-17A treatment improved survival, with the survival rate increasing from 0% in the isotype control group to 60% (P = 0.011; **Figure 6**). This further

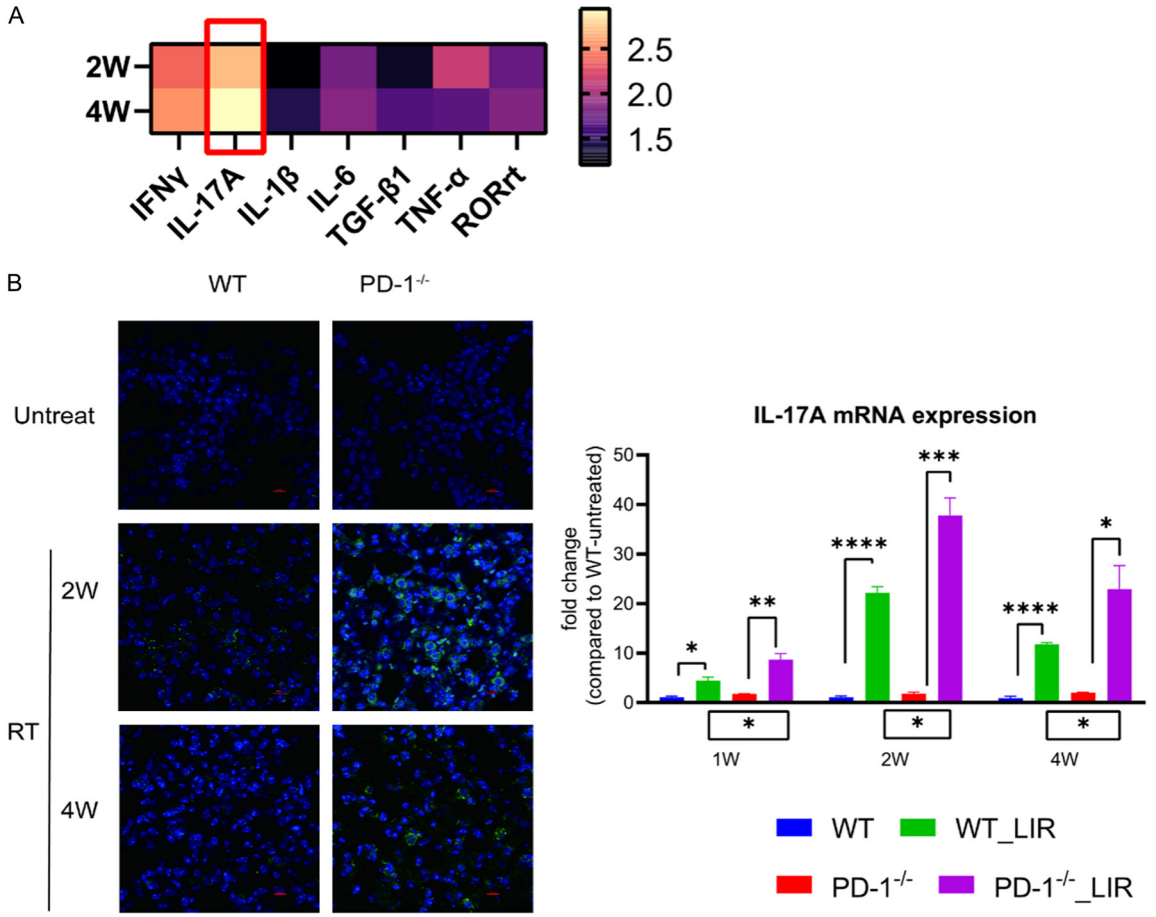

Figure 3. Changes in IL-17A immunofluorescence and mRNA expression levels in mouse lung tissue after radiotherapy. A. Differential heatmap of gene expression for various immune-related genes at weeks 2 and 4 post-radiation in PD-1$^{-/-}$ group compared to WT group. B. Immunofluorescence was used to detect changes in IL-17A expression in PD-1 deficient and WT mice at baseline, 2 weeks post-radiotherapy, and 4 weeks post-radiotherapy. Right: Changes in IL-17A mRNA expression levels in mouse lung tissue following radiotherapy. Fold change data are presented as mean ± SEM. *P* values (ns, not significant; *P < 0.05; **P < 0.01; ***P < 0.001; ****P < 0.0001) were determined by two-tailed t-test.

underscores the significant positive impact of αIL-17A treatment on mouse survival. Our study also revealed that although at the initial stages, there was no significant difference in survival rates between WT mice and PD-1$^{-/-}$ mice, after radiation therapy, PD-1$^{-/-}$ mice displayed a significantly decreased survival rate. This finding emphasizes the sensitivity of PD-1$^{-/-}$ mice to radiation therapy and confirms the significant role of αIL-17A treatment in improving mouse survival. In summary, our experiments demonstrate that αIL-17A can inhibit the secretion of inflammatory cytokines and chemokines, as well as the infiltration of CD8^{+} or CD4^{+} T cells in mouse lung tissue induced by radiation therapy combined with αPD-1.

Discussion

In this study, we aimed to investigate the safety of concurrent radiotherapy (RT) and αPD-1 immunotherapy using a radiation-induced lung injury (RILI) mouse model. Our results indicate that concomitant RT in the absence of PD-1 aggravates the severity of RILI. Further analysis revealed that the combination of αPD-1 antibody and RT resulted in a significant increase in IL-17A expression, which exacerbated acute RILI. However, RILI was reduced when αIL-17A was used. While immune checkpoint inhibitors have been approved for lung cancer treatment, their combination with radiotherapy and immunotherapy may result in worsened lung injury after radiotherapy. In our study, we examined the effect of combined chest radiotherapy and

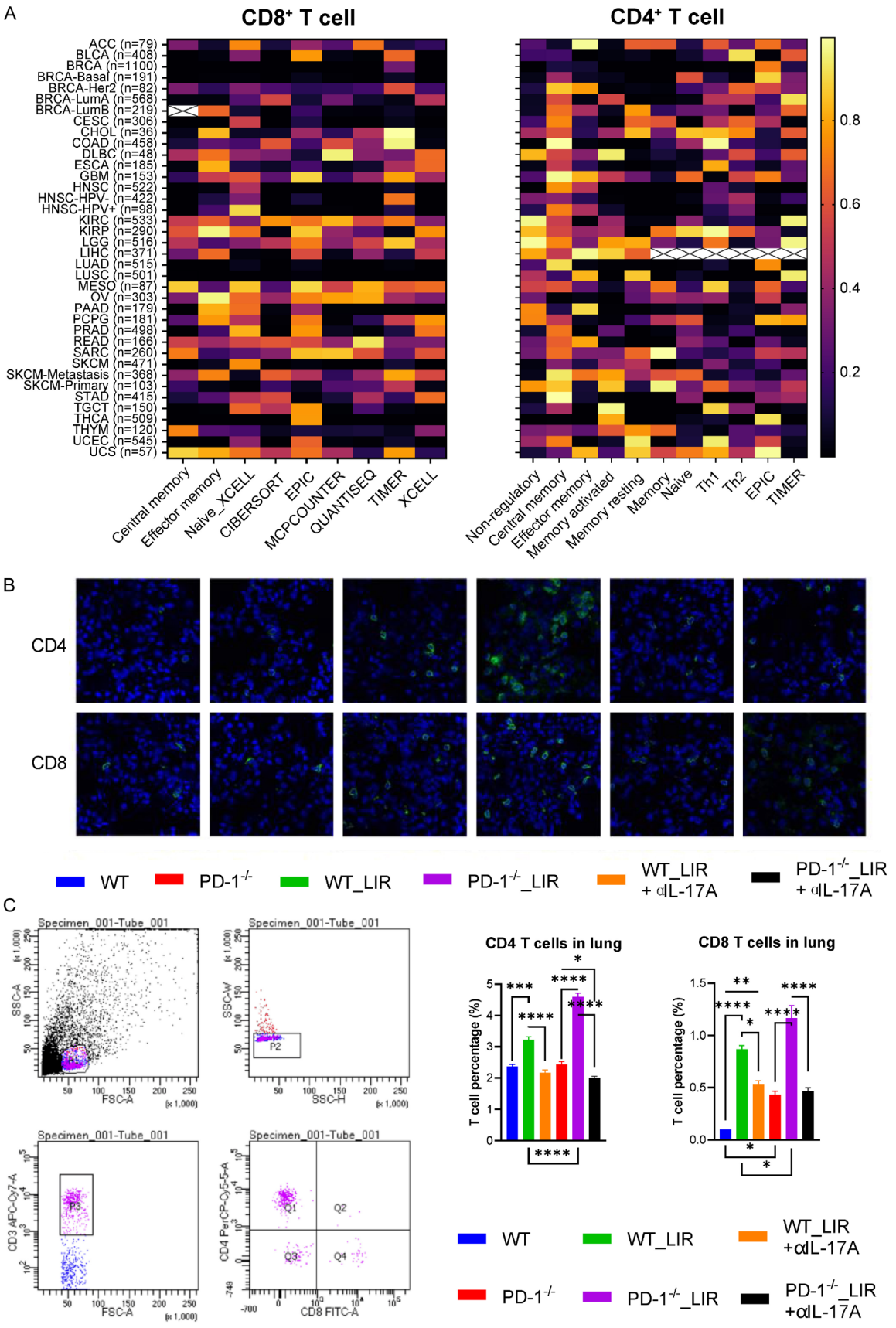
A
CD8+ T cell
CD4+ T cell
ACC (n=79)
BLCA (n=408)
BRCA (n=1100)
BRCA-Basal (n=191)
BRCA-Her2 (n=82)
BRCA-LumA (n=568)
BRCA-LumB (n=219)
CESC (n=306)
CHOL (n=36)
COAD (n=458)
DLBC (n=48)
ESCA (n=185)
GBM (n=153)
HNSC (n=522)
HNSC-HPV- (n=422)
HNSC-HPV+ (n=98)
KIRC (n=533)
KIRP (n=290)
LGG (n=516)
LIHC (n=371)
LUAD (n=515)
LUSC (n=501)
MESO (n=87)
OV (n=303)
PAAD (n=179)
PCPG (n=181)
PRAD (n=498)
READ (n=166)
SARC (n=260)
SKCM (n=471)
SKCM-Metastasis (n=368)
SKCM-Primary (n=103)
STAD (n=415)
TGCT (n=150)
THCA (n=509)
THYM (n=120)
UCEC (n=545)
UCS (n=57)
0.8
0.6
0.4
0.2
Central memory
Effector memory
Naive _XCELL
CIBERSORT
EPIC
MCPCOUNTER
QUANTISEQ
TIMER
XCELL
Non-regulatory
Central memory
Effector memory
Memory activated
Memory resting
Memory
Naive
Th1
Th2
EPIC
TIMER
B
CD4
CD8
WT
PD-1-/-
WT_LIR
PD-1-/-_LIR
WT_LIR + αIL-17A
PD-1-/-_LIR + αIL-17A
C
Specimen_001-Tube_001
SSC-A
FSC-A
SSC-H
SSC-W
P1
P2
CD3 APC-Cy7-A
CD4 PerCP-Cy5-5-A
CD8 FITC-A
P3
Q1
Q2
Q3
Q4
CD4 T cells in lung
CD8 T cells in lung
T cell percentage (%)
WT
WT_LIR
WT_LIR +αIL-17A
PD-1-/-
PD-1-/-_LIR
PD-1-/-_LIR +αIL-17A

Figure 4. Changes in CD4 and CD8 immune-related cells in mouse lung tissue. A. TIMER based spearman correlational analysis between the expression of IL17A genes, $CD8^+$ and $CD4^+$ T immune cell infiltration. B. Immunofluorescence was used to measure the expression changes of $CD4^+$ and $CD8^+$ T cells in each group at 2 weeks after radiotherapy. C. Flow cytometry was used to measure the percents of $CD4^+$ or $CD8^+$ cells in mouse lung tissue. Fold change data are presented as mean ± SEM. *P* values (ns, not significant; **P* < 0.05; ***P* < 0.01; ****P* < 0.001; *****P* < 0.0001) were determined by one-way ANOVA.

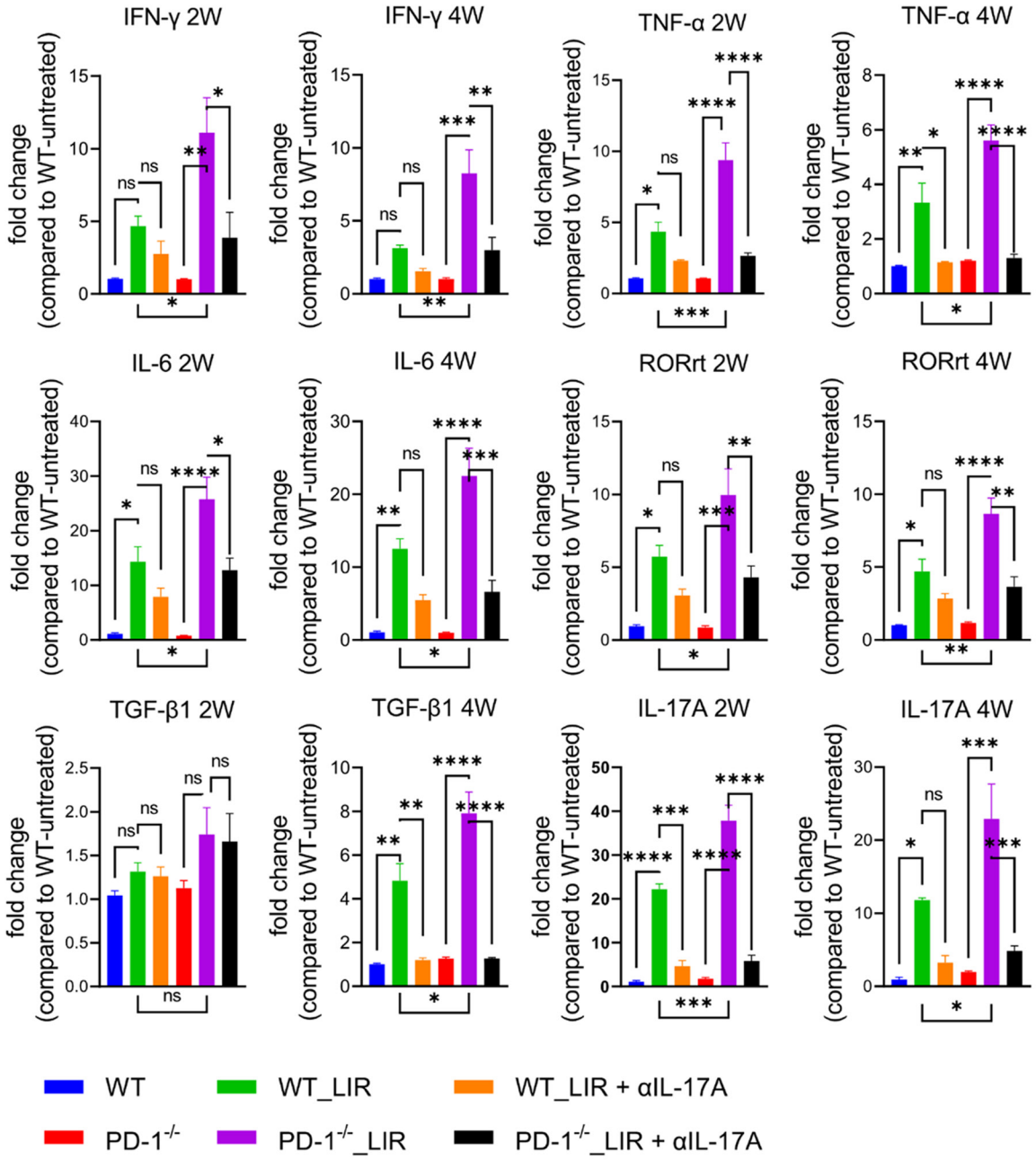

Figure 5. Changes in immune-related factors in mouse lung tissue after RILI. qPCR was used to measure the changes in immune-related factors in mouse lung tissue at 2/4 weeks after radiotherapy. Fold change data are presented as mean ± SEM. *P* values (ns, not significant; **P* < 0.05; ***P* < 0.01; ****P* < 0.001; *****P* < 0.0001) were determined by one-way ANOVA.

αIL-17A therapy to understand how this combination affects non-malignant lung tissue.

RILI is characterized by the destruction of lung structures and a sequence of inflammatory

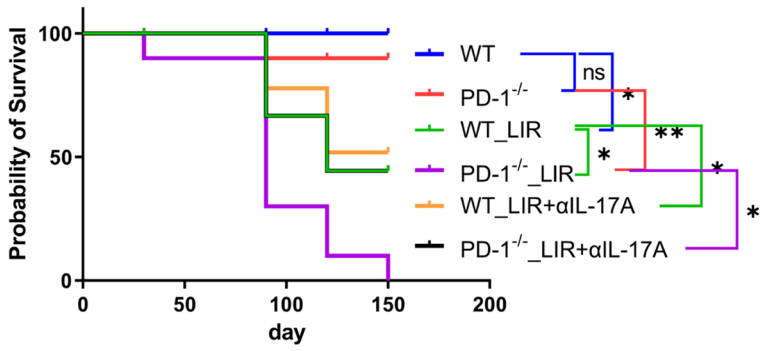

Figure 6. Survival curve of mice. Survival status of mice in each group after radiotherapy, with 10 mice in each group. *P* values (ns, not significant; **P* < 0.05; ***P* < 0.01; ****P* < 0.001; *****P* < 0.0001) were determined by log-rank test.

events that involve the recruitment of diverse immune cells and a continuous cascade of cytokines and chemokines [24]. In accordance with prior studies, leukocytes were observed to infiltrate the lungs in a time-dependent manner after irradiation, likely in response to acute radiation-induced effects such as DNA damage, reactive oxygen species (ROS) generation, and apoptosis [15, 24]. In the presence of αPD-1 antibodies or PD-1$^{-/-}$, radiation-induced inflammatory cell infiltration in the lung tissue was increased, leading to worsened histopathological changes.

PD-1 deficiency leads to reduced T cell proliferation, production of IFN, TNF, IL-2, and impaired T cell survival. PD-1 expression serves as a marker of "exhausted" T cells, a condition often triggered by high levels of stimulation or reduced CD4$^+$ T cell help [25]. This exhaustion occurs in chronic infections and cancer, resulting in suboptimal control of infections and tumors. Within the tumor microenvironment (TME), tumor cells expressing PD-L1 promote T cell apoptosis and weaken the immune system's ability to eliminate tumor cells. PD-1 knockout mice exhibit autoimmunity due to the breakdown of peripheral tolerance [26, 27]. RT has been demonstrated to enhance antitumor immune responses by altering tumor phenotypes, rendering them more susceptible to cytotoxic T lymphocyte (CTL) killing [28]. However, the activity of CTLs can be limited by suppressive regulatory T cells (Tregs). The direct effects of radiation on Treg biology remain controversial. Hence, the blockade of IL-17A is currently undergoing testing in both preclinical and clinical settings. Recent studies have demonstrated that the combined treatment involving IL-17A blockade, along with anti-PD-1 blockade, has resulted in a significant reduction in the proliferation of CD4$^+$ and CD8$^+$ T cells in the context of cancer as well as lung architecture [13, 29]. Our findings indicate that exposure to ionizing radiation results in an increased proportion of CD8$^+$ and CD4$^+$ T cells in lung tissue. Therefore, further investigation on the effect of IL-17A blockade on tumors is urgently needed.

IL-17A stimulates various cell types to produce pro-inflammatory cytokines, such as IL-1, IL-6, IL-8, IL-10, IL-12, and TNF-α, creating an IL-17A-based cytokine network to participate in inflammation [12, 15]. These cytokines recruit immune cells such as lymphocytes and neutrophils, promoting fibroblast activation and collagen synthesis, ultimately leading to fibrosis. Th17 cells are associated with radiation-induced lung fibrosis in mouse models, and IL-17 plays a crucial role in radiation-induced lung injury [13]. During pneumonia, TH1-type pro-inflammatory cytokines are secreted during the early stage, and both TH1 and TH17 cells participate in the pro-inflammatory response [30, 31]. αIL-17A can significantly reduce radiation-induced pulmonary fibrosis and increase the survival period of irradiated mice by modulating cytokines IL-6 and TGF-β [32, 33].

In our study, we found that concurrent deletion of the PD-1 gene led to an increase in the infiltration of IL-17A-producing CD4$^+$ and CD8$^+$ T cells in irradiated lungs at days 14 after irradiation. The levels of IL-17A in the PD-1$^{-/-}$ + LIR group gradually increased, peaking at day 14 post-irradiation and remaining high at day 28 post-irradiation. IL-17A plays a critical role in attracting myeloid cells, such as neutrophils, to the injured tissue. Deletion of the PD-1 gene significantly increased the number of neutrophils in lung tissue at day 14 and day 28 after irradiation.

In summary, our study suggests that the concurrent administration of αPD-1 treatment and irradiation can lead to an increase in the infiltration of IL-17A-producing cells in lung tissue

and an increase in neutrophil recruitment, which may contribute to lung injury. However, in this study, we only performed *in vivo* experiments in mice and the mechanism still warrants further research. In the future, more clinical study will be considered.

Acknowledgements

This work was supported by Beijing Medical Award Foundation Project (YXJL-2020-0961-0159).

Disclosure of conflict of interest

None.

Address correspondence to: Songliu Hu, Department of Radiation Oncology, Harbin Medical University Cancer Hospital, No. 150 Haping Road, Nangang District, Harbin 150081, Heilongjiang, China. Tel: +86-0451-86298521; E-mail: drhusongliu@163.com

References

[1] Cytlak UM, Dyer DP, Honeychurch J, Williams KJ, Travis MA and Illidge TM. Immunomodulation by radiotherapy in tumour control and normal tissue toxicity. Nat Rev Immunol 2022; 22: 124-138.

[2] Liu T, Yang Q, Zheng H, Jia H, He Y, Zhang X, Zheng J, Xi Y, Zhang H, Sun R, Chen X and Shan W. Multifaceted roles of a bioengineered nanoreactor in repressing radiation-induced lung injury. Biomaterials 2021; 277: 121103.

[3] Madani I, De Ruyck K, Goeminne H, De Neve W, Thierens H and Van Meerbeeck J. Predicting risk of radiation-induced lung injury. J Thorac Oncol 2007; 2: 864-874.

[4] Hanania AN, Mainwaring W, Ghebre YT, Hanania NA and Ludwig M. Radiation-induced lung injury: assessment and management. Chest 2019; 156: 150-162.

[5] Davies MJ. PD-1/PD-L1 inhibitors for non-small cell lung cancer: incorporating care step pathways for effective side-effect management. J Adv Pract Oncol 2019; 10 Suppl 1: 21-35.

[6] Zhao B, Li H and Ma W. Durvalumab after chemoradiotherapy for patients with unresectable stage III NSCLC: the PACIFIC-R study. J Thorac Oncol 2023; 18: e38-e39.

[7] Theelen WSME, Peulen HMU, Lalezari F, van der Noort V, de Vries JF, Aerts JGJV, Dumoulin DW, Bahce I, Niemeijer AN, de Langen AJ, Monkhorst K and Baas P. Effect of pembrolizumab after stereotactic body radiotherapy vs pembrolizumab alone on tumor response in patients with advanced non-small cell lung cancer: results of the PEMBRO-RT phase 2 randomized clinical trial. JAMA Oncol 2019; 5: 1276-1282.

[8] Reck M, Rodríguez-Abreu D, Robinson AG, Hui R, Csőszi T, Fülöp A, Gottfried M, Peled N, Tafreshi A, Cuffe S, O'Brien M, Rao S, Hotta K, Leiby MA, Lubiniecki GM, Shentu Y, Rangwala R and Brahmer JR; KEYNOTE-024 Investigators. Pembrolizumab versus chemotherapy for PD-L1-positive non-small-cell lung cancer. N Engl J Med 2016; 375: 1823-1833.

[9] Antonia SJ, Villegas A, Daniel D, Vicente D, Murakami S, Hui R, Yokoi T, Chiappori A, Lee KH, de Wit M, Cho BC, Bourhaba M, Quantin X, Tokito T, Mekhail T, Planchard D, Kim YC, Karapetis CS, Hiret S, Ostoros G, Kubota K, Gray JE, Paz-Ares L, de Castro Carpeño J, Wadsworth C, Melillo G, Jiang H, Huang Y, Dennis PA and Özgüroğlu M; PACIFIC Investigators. Durvalumab after chemoradiotherapy in stage III non-small-cell lung cancer. N Engl J Med 2017; 377: 1919-1929.

[10] Jabbour SK, Cho BC, Bria E, Kato T, Bhosle J, Gainor JF, Reguart N, Wang L, Morgensztern D, Shentu Y, Kim SJ, Souza F and Reck M. Rationale and design of the phase III KEYLYNK-012 study of pembrolizumab and concurrent chemoradiotherapy followed by pembrolizumab with or without olaparib for stage III non-small-cell lung cancer. Clin Lung Cancer 2022; 23: e342-e346.

[11] Jabbour SK, Lee KH, Frost N, Breder V, Kowalski DM, Pollock T, Levchenko E, Reguart N, Martinez-Marti A, Houghton B, Paoli JB, Safina S, Park K, Komiya T, Sanford A, Boolell V, Liu H, Samkari A, Keller SM and Reck M. Pembrolizumab plus concurrent chemoradiation therapy in patients with unresectable, locally advanced, stage III non-small cell lung cancer: the phase 2 KEYNOTE-799 nonrandomized trial. JAMA Oncol 2021; 7: 1-9.

[12] Ott PA, Elez E, Hiret S, Kim DW, Morosky A, Saraf S, Piperdi B and Mehnert JM. Pembrolizumab in patients with extensive-stage small-cell lung cancer: results from the phase Ib KEYNOTE-028 study. J Clin Oncol 2017; 35: 3823-3829.

[13] Sheng Y, Chen K, Jiang W, Wu Z, Zhang W, Jing H, Wang L, Qu C and Ren H. PD-1 restrains IL-17A production from γδ T cells to modulate acute radiation-induced lung injury. Transl Lung Cancer Res 2021; 10: 685-698.

[14] Garg AD, De Ruysscher D and Agostinis P. Immunological metagene signatures derived from immunogenic cancer cell death associate with improved survival of patients with lung, breast or ovarian malignancies: a large-scale

meta-analysis. Oncoimmunology 2015; 5: e1069938.
[15] Mills KHG. IL-17 and IL-17-producing cells in protection versus pathology. Nat Rev Immunol 2023; 23: 38-54.
[16] Wang YN, Lou DF, Li DY, Jiang W, Dong JY, Gao W and Chen HC. Elevated levels of IL-17A and IL-35 in plasma and bronchoalveolar lavage fluid are associated with checkpoint inhibitor pneumonitis in patients with non-small cell lung cancer. Oncol Lett 2020; 20: 611-622.
[17] Du S, Zhou L, Alexander GS, Park K, Yang L, Wang N, Zaorsky NG, Ma X, Wang Y, Dicker AP and Lu B. PD-1 modulates radiation-induced cardiac toxicity through cytotoxic T lymphocytes. J Thorac Oncol 2018; 13: 510-520.
[18] Kuwano K, Hagimoto N, Kawasaki M, Yatomi T, Nakamura N, Nagata S, Suda T, Kunitake R, Maeyama T, Miyazaki H and Hara N. Essential roles of the Fas-Fas ligand pathway in the development of pulmonary fibrosis. J Clin Invest 1999; 104: 13-19.
[19] Krüse JJ, Zurcher C, Strootman EG, Bart CI, Schlagwein N, Leer JW and Wondergem J. Structural changes in the auricles of the rat heart after local ionizing irradiation. Radiother Oncol 2001; 58: 303-311.
[20] Li B, Severson E, Pignon JC, Zhao H, Li T, Novak J, Jiang P, Shen H, Aster JC, Rodig S, Signoretti S, Liu JS and Liu XS. Comprehensive analyses of tumor immunity: implications for cancer immunotherapy. Genome Biol 2016; 17: 174.
[21] Li T, Fan J, Wang B, Traugh N, Chen Q, Liu JS, Li B and Liu XS. TIMER: a web server for comprehensive analysis of tumor-infiltrating immune cells. Cancer Res 2017; 77: e108-e110.
[22] Zhou Y, Zhou B, Pache L, Chang M, Khodabakhshi AH, Tanaseichuk O, Benner C and Chanda SK. Metascape provides a biologist-oriented resource for the analysis of systems-level datasets. Nat Commun 2019; 10: 1523.
[23] Sheng Y, Chen K, Jiang W, Wu Z, Zhang W, Jing H, Wang L, Qu C and Ren H. PD-1 restrains IL-17A production from γδ T cells to modulate acute radiation-induced lung injury. Transl Lung Cancer Res 2021; 10: 685-698.
[24] Schaue D and McBride WH. T lymphocytes and normal tissue responses to radiation. Front Oncol 2012; 2: 119.
[25] Niborski LL, Gueguen P, Ye M, Thiolat A, Ramos RN, Caudana P, Denizeau J, Colombeau L, Rodriguez R, Goudot C, Luccarini JM, Soudé A, Bournique B, Broqua P, Pace L, Baulande S, Sedlik C, Quivy JP, Almouzni G, Cohen JL, Zueva E, Waterfall JJ, Amigorena S and Piaggio E. CD8+T cell responsiveness to anti-PD-1 is epigenetically regulated by Suv39h1 in melanomas. Nat Commun 2022; 13: 3739.
[26] Sharpe AH and Pauken KE. The diverse functions of the PD1 inhibitory pathway. Nat Rev Immunol 2018; 18: 153-167.
[27] Mi Y, Han J, Zhu J and Jin T. Role of the PD-1/PD-L1 signaling in multiple sclerosis and experimental autoimmune encephalomyelitis: recent insights and future directions. Mol Neurobiol 2021; 58: 6249-6271.
[28] Zhang Z, Liu X, Chen D and Yu J. Radiotherapy combined with immunotherapy: the dawn of cancer treatment. Signal Transduct Target Ther 2022; 7: 258.
[29] Celada LJ, Kropski JA, Herazo-Maya JD, Luo W, Creecy A, Abad AT, Chioma OS, Lee G, Hassell NE, Shaginurova GI, Wang Y, Johnson JE, Kerrigan A, Mason WR, Baughman RP, Ayers GD, Bernard GR, Culver DA, Montgomery CG, Maher TM, Molyneaux PL, Noth I, Mutsaers SE, Prele CM, Peebles RS Jr, Newcomb DC, Kaminski N, Blackwell TS, Van Kaer L and Drake WP. PD-1 up-regulation on CD4(+) T cells promotes pulmonary fibrosis through STAT3-mediated IL-17A and TGF-β1 production. Sci Transl Med 2018; 10: eaar8356.
[30] Dardalhon V, Korn T, Kuchroo VK and Anderson AC. Role of Th1 and Th17 cells in organ-specific autoimmunity. J Autoimmun 2008; 31: 252-256.
[31] Kajdaniuk D, Foltyn W, Morawiec-Szymonik E, Czuba Z, Szymonik E, Kos-Kudła B and Marek B. Th17 cytokines and factors modulating their activity in patients with pernicious anemia. Immunol Res 2023; 71: 873-882.
[32] Baldeviano GC, Barin JG, Talor MV, Srinivasan S, Bedja D, Zheng D, Gabrielson K, Iwakura Y, Rose NR and Cihakova D. Interleukin-17A is dispensable for myocarditis but essential for the progression to dilated cardiomyopathy. Circ Res 2010; 106: 1646-1655.
[33] Martinu T, McManigle WC, Kelly FL, Nelson ME, Sun J, Zhang HL, Kolls JK, Gowdy KM and Palmer SM. IL-17A contributes to lung fibrosis in a model of chronic pulmonary graft-versus-host disease. Transplantation 2019; 103: 2264-2274.